Response Surface Approximations for Aerodynamic Parameters in High Speed Civil Transport Optimization

Oleg B. Golovidov*, William H. Mason†,
Bernard Grossman‡, Layne T. Watson§, Raphael T. Haftka¶

Multidisciplinary Analysis and Design (MAD) Center for Advanced Vehicles
Virginia Polytechnic Institute and State University
Blacksburg, Virginia 24061

Abstract

A procedure for generating and using polynomial approximations to the range or to the cruise drag components in terms of 29 design variables for a High Speed Civil Transport configuration design is presented. Response surface methodology is used to fit quadratic polynomials to data gathered from a series of numerical analyses of different aircraft designs. Several techniques are employed to minimize the number of required analyses and to maintain accuracy. Approximate analysis techniques are used to find regions of the design space where reasonable aircraft designs could occur and response surface models are built using higher fidelity analysis results of the designs in this "reasonable" region. This is a means of using results from advanced CFD methods at the early design stage. Regression analysis and analysis of variance are used to reduce the number of polynomial terms in the response surface model functions. Optimization runs of the aircraft configuration are then carried out with the response surface models and compared to the previous optimization runs without the response surface models. It is shown that considerable reduction of the amount of numerical noise in optimization is achieved with response surface models and the convergence rate is improved. Careful attention was required to keep the accuracy of the models at an acceptable level.

1. Introduction

Response surface methodology (RSM) [1, 2, 3] uses simple mathematical models (e.g., low-order polynomials or other simple basis functions) to approximate the *response* of a computationally expensive analysis tool during the optimization process. Such response

*Graduate Research Assistant, Dept. of Aerospace and Ocean Engineering, Student Member AIAA
†Professor of Aerospace and Ocean Engineering, Associate Fellow AIAA
‡Professor and Head, Dept. of Aerospace and Ocean Engineering, Associate Fellow AIAA
§Professor of Computer Science and Mathematics
¶Professor of Aerospace Engineering, Mechanics and Engineering Science, University of Florida, Gainesville, FL, 32611, Fellow AIAA

surface models are created using a limited number of analyses at a set of statistically selected points in the design space. Selection of designs for creating response surface (RS) models using *design of experiments theory* (DOE) [4] attempts to achieve maximum accuracy using a minimal number of designs. Using RSM in optimization helps to solve several problems in multidisciplinary design optimization (MDO): adverse effects of numerical noise of high fidelity analysis tools, their extremely high computational cost which makes them difficult to use directly in the MDO process, the strong possibility of getting trapped in multiple local optima due to the presence of numerical noise. There are also other advantages: fast design evaluation, a shortened optimization process, and inexpensive trade-off studies.

RSM has been used traditionally in optimization with a small number of design variables. First applications of the RSM and DOE methods for aerodynamic optimization can be dated as far back as 1964, when Powers [5] used approximations to find the minimum drag body shape. In recent years considerable interest has been shown in the use of RSM methods in MDO problems. Some examples of such studies are given in the works by Tai, *et al.* [6] Sellar, *et al.* [7] and Engelund, *et al.* [8]. In the MDO of a High-Speed Civil Transport (HSCT), the RSM was used by Giunta, *et al.* [9, 10, 11] to construct approximations to aerodynamic drag in two, five, and ten design variables.

As the dimensionality of the design space increases, so does the complexity of the problem of RSM application. Each additional dimension increases the volume of the design space considerably. The so-called *curse of dimensionality* makes full factorial experimental designs impossible in high dimensions, and partial factorial or other experimental designs (D-optimal) have to be used, so that the design space sampling is very sparse. Even with the increased number of design samples to define the higher order approximation model, the accuracy of the model is often poor in high dimensional space.

In this work we extend the RSM approach to the ambitious number of 29 design variables to build approximations for the range and drag related coefficients of the HSCT. The range constraint is one of the most important HSCT constraints affecting the configuration of the aircraft. Approximations to the drag components were used as an alternative way to model the range of an HSCT, since the cruise drag directly affects the range. We used the *reasonable design space* approach to control the accuracy of the models. This included screening of the candidate designs and using side constraints on the design variables. Also, updating the data set with the intermediate designs was used to improve the accuracy. A detailed description of the studies can be found in Ref. [12].

Section 2 describes the HSCT design problem to which RSM is applied in this work. In section 3 the process of creating response surface models is described in some detail. Sections

4 and 5 describe the results of generation of the RS models and their implementation in an HSCT optimization. Conclusions are offered in section 6.

2. The HSCT Design Problem, Methods, and Optimization Approach

The HSCT design problem [13, 14] that we address is to optimize an aircraft configuration to minimize take-off gross weight (TOGW) for a range of 5500 n.mi., and 251 passengers. The aircraft's mission is a supersonic cruise-climb at Mach 2.4 with a maximum altitude of 70,000 *ft*.

TOGW was chosen as the merit function due to its direct relation to the aerodynamic, structural, and propulsion efficiency of the aircraft. Structural design of the aircraft dictates its empty weight, while aerodynamic performance affects the required amount of fuel weight. Both components contribute to the TOGW and determine the required engine size.

2.1. Design Variables

To perform the numerical optimization of an HSCT configuration, the latter has to be completely and uniquely described by a set of design variables. In our problem, an HSCT configuration has been parametrized by 29 design variables uniquely describing the aircraft's geometry, propulsion system, and mission.

The variables can be divided into seven categories: wing planform, airfoil, nacelle placement, engine thrust, fuselage shape, mission performance variables, and tail areas. The eight design parameters used to define the planform are shown in Fig. 1. The leading and trailing edges of the wing are defined using a blending of linear segments.

The airfoil sections have round leading edges. We define the thickness distribution using an analytic description [15]. It is defined by four parameters: the thickness-to-chord ratio t/c, the leading-edge radius parameter I, the chordwise location of maximum thickness m, and the trailing-edge half angle τ_{TE}; see Fig. 1.

Three variables define the idealized cruise mission. One variable is the mission fuel and the other two specify the Mach 2.4 cruise in terms of the initial supersonic cruise altitude and the constant climb rate used in the range calculation. The resulting aircraft range is calculated using the fuel weight design variable, assuming that 85% of the mission fuel is used in cruise and the remaining 15% is the reserve fuel. See Ref. [13] for the full list of design variables.

2.2. Constraints

The constraints used in the problem fall into three categories: constraints implicit in the analysis, performance/aerodynamic constraints, and geometric constraints. The implicit constraints are not handled by the optimization program, but rather are part of the analysis or geometry:

1. The maximum altitude, 70,000 *ft*, is enforced in the range calculation.
2. The fuselage volume is fixed at 23,270 ft^3 and the fuselage length is fixed at 300 *ft*.
3. The axial location of the 25% of the wing's mean aerodynamic chord is adjusted to match the value found on the baseline configuration (147.3 *ft* aft of the aircraft nose).
4. The nacelles are fixed axially with a 25% overhang.

Aside from these implicit constraints we also use 68 explicit constraints, described in detail in Ref. [13]. They include aerodynamic, mission performance, trim and control, and geometric constraints aimed at preventing the optimizer from developing infeasible and/or geometrically impossible designs. Aerodynamic constraints include the range requirement (5500 n.mi.), restrictions on maximum lift coefficient and landing angle of attack. Engine and wing tip scrape constraints prevent ground strike during landing. Geometrical constraints prevent physically impossible designs, e.g., they require the outboard nacelle be outside of the inboard one, the wing not overlaping the tail, etc. Trim and control constraints require that the aircraft have sufficient control authority for trim and maneuvers without exceeding the limits on the deflection angles of the tail surfaces. Thrust constraints require the available engine thrust to be greater than the required thrust.

2.3. Optimization Approach

A complete design optimization is composed of a sequence of optimization cycles. In our so-called "standard" MDO procedure without use of RS models, detailed analysis methods are employed at the beginning of each cycle, while simple analyses, scaled to match the initial detailed results, are performed in subsequent calculations during each cycle. We call this *variable-complexity methodology* [13, 16, 17]. A typical HSCT design requires approximately 40–50 cycles until an optimal configuration is identified. The optimizer NEWSUMT-A [18], which employs an extended interior penalty function method, is used for this work. NEWSUMT-A utilizes constraints based on both the simple and detailed analyses along with constraints that limit the movement of the design variables. Move limits are imposed on the design variables on each optimization cycle, so that the optimizer is always in the region of the design space where the scaling factors are valid.

2.4. Analysis Methods

We use the aerodynamic drag analysis methods and representation of the wing structure with weight equations as described in Refs. [19, 20, 21]. The so-called "exact" or high fidelity aerodynamics calculations used in this work are based on the vortex lattice method [22], the Mach box method [23, 24], and the Harris wave drag code [25]. A simple strip boundary layer skin friction estimate is implemented as in Ref. [20].

The simplified or "approximate" methods of aerodynamic analysis used in this work include wave drag estimation using a classical far-field slender body formulation as implemented by Hutchison [26], with the oblique cross-section calculations replaced by the use of normal areas to reduce the computational time. A simplified calculation of the drag due to lift is based on the cranked delta wing method as described in [21]; analytical solutions for these wings have been given in the work by Cohen and Friedman [27]. A detailed description of the analysis methods used is given in Ref. [13].

3. Response Surface Model Generation Process

The RSM approach used in this work is based primarily on the work done by Kaufman [28], who developed the algorithms and used RSM to incorporate the results of structural optimizations of the wing bending material weight into the HSCT optimization process [29]. Quadratic polynomials are used for response surface models in this work, so that for p design variables, a model will have $n = (p+1)(p+2)/2$ terms. In such a model the polynomial coefficients may be estimated using the method of least squares. For 29 design variables this yields a quadratic polynomial with 465 terms.

3.1. Creating a Central Design

The RSM process begins with creation of a *central* (or *baseline*) design which is that reference point in the multivariable design space around which a *reasonable design space* will be created. By *reasonable designs*, we mean those designs having similar characteristics to the feasible designs even though some of the aerodynamic and performance constraints may be violated (discussed later).

To ensure that a large part of the design space used for creating RS models lies in the feasible domain, it is preferable to have the central design *inside* the feasible domain. For this investigation, this was accomplished by performing a "standard" optimization with constraints *tightened* by 1–2%. This produced the feasible, although not optimum (heavy), design used as the baseline. Figure 2 shows two views of the baseline configuration.

3.2. Initial Design Space Generation

The next step of the RSM process is the generation of a large number of candidate designs covering that portion of the design space where the models are expected to be valid. The approach used in this work is based on the partially balanced incomplete block design ([30], pp. 297–299) of order three. In this algorithm, implemented in the *HSCTSearch* code by Kaufman, up to three scaled design variables per design point are allowed to take values $\{-1, +1\}$, while the rest of the variables are held constant at the third level 0. For twenty nine design variables this requires 30,915 points. All 29 variables were varied by $\pm 20\%$ of the value of the central design. This perturbation amount was expected to permit accurate representation of the actual response by quadratic polynomials based on the previous experience with the magnitude of design variation.

3.3. Identification of the Reasonable Design Space

Generation of the initial design space is followed by the reduction of its volume to the size of the reasonable design space, containing reasonable HSCT configurations and excluding unrealistic designs from consideration. The set of constraints, used to determine whether a design is reasonable or not (see Table 1), includes 34 standard geometric constraints for the HSCT, several additional geometric constraints and some aerodynamic constraints which use "approximate" methods for design analysis and are therefore inexpensive to evaluate. The elimination of unreasonable designs was not possible, since this would have resulted in removing most of the designs in the already very sparsely covered design space. Instead, each unreasonable design $\mathbf{x}$ was moved along a straight line towards the baseline design $\mathbf{x}_c$ until it met all of the criteria. This procedure brings an unreasonable design $\mathbf{x}$ to the border of the reasonable design space, using a parameter β as:

$$\mathbf{x}' = \beta\,(\mathbf{x} - \mathbf{x}_c) + \mathbf{x}_c\,. \tag{1}$$

The parameter β, $0 \leq \beta \leq 1$, was found for each design using bisection with tolerance 0.01.

3.4. Selection of D-optimal Designs

Even though we limited the reasonable design space to a much smaller number of designs than a full factorial design, the computational expense of performing high fidelity HSCT analyses on each reasonable design is still enormous, as is the expense of doing a regression analysis on the full set of 30,915 designs. Therefore, a subset of the designs is used to perform the high fidelity analyses used in response surface model generation. Previous experience [28] indicated that the ratio of the number of designs to the number of coefficients in the model should be at least 3 for a high number of design variables (25–29) to reliably fit a quadratic polynomial to the analysis results.

The D-optimality criterion [31] was used for selecting the subset. The *Dopt* code written by D. Haim was used to select the specific designs. This code utilizes the "k-exchange" method of Mitchell [32] for selection of the D-optimal set of designs.

Two sets of designs were chosen: set A of 1446 designs for generating the RS models, and set B of 1426 designs for checking the accuracy. D-optimality was not fully achieved due to the large computational expense. About 400 iterations were made for each data set. Although the D-efficiency values were low, on the order of 1%, the condition numbers of the $\mathbf{X}$-matrices (252 for data set A and 113 for data set B, using scaled design variables) were sufficiently good to prevent ill-conditioning of the least squares problem, described next.

3.5. Response Surface Model Generation Using Regression Analysis and ANOVA

The *RSG* code [28] written by Kaufman was used for creating the RS models. The SVD algorithm from the LAPACK library [33] was used for the least squares fit. To prevent ill-conditioning, all data in both data sets were scaled to be between -1 and 1, based on data set A (used for generating the response surface models), before any RS models were generated.

Regression analysis, along with the polynomial coefficients, also provides a measure of the uncertainty in these coefficients. Analysis of variance (ANOVA) ([3], p.28) involves estimating the variance of the predicted polynomial coefficients. Terms in the polynomial model having large coefficients of variation, typically over 0.10, may be dropped from the polynomial without significantly affecting the fidelity of the response surface fit.

The *RSG* code allows the user to perform a so-called one-step backwards regression, where the term with the highest coefficient of variation is removed from the model function, and the process of regression analysis and ANOVA is repeated until a certain stopping criterion is reached (e.g., a minimum number of terms specified by the user). This is an essential step in the response surface model generation process, as it not only reduces the complexity of the model function considerably, but also improves the prediction accuracy of the model, as will be shown below.

4. Generation of Range and Drag Components' Response Surface Models

Two alternative ways of approximating the range of the HSCT are considered here: first, an RS model of the HSCT range as a function of the design variables is constructed, and second, three RS models of the cruise drag related coefficients — wave drag coefficient $C_{D_{wave}}$, lift curve slope C_{L_α}, and leading edge suction term C_T/C_L^2 — are constructed, and the range is calculated using the approximation models to these coefficients. Thus, 4 response surface models — for the range of the HSCT, $C_{D_{wave}}$, C_{L_α}, and C_T/C_L^2 — were generated. All RS models were generated using data set A and errors checked at data points of set B in each case. Using the *RSG* code, one-step backwards regression (Section 3.5) was performed to get the error for each response surface model versus the number of coefficients in the model polynomial. The prediction errors (computed on data set B) for the range response surface model are plotted in Figure 3.

Notice that the prediction errors decrease with the reduction in the number of polynomial terms, down to approximately 130–150 terms, where most of the unreliable terms have been removed. The majority of the discarded terms are second order interactions that did not have a large effect on the range or were difficult to define using the available information in data set A. Among the linear terms discarded were some of the fuselage design variables, leading edge radius parameter, and nacelle 1 position. Further polynomial reduction leads to losses of information and increases the prediction errors. The optimum number of terms, judging by Figure 3, is about 130–150. Thus, a 150 term polynomial was chosen for the range response surface model.

A similar effect was observed for the RS models of the drag components. For each response surface model the optimum number of terms in the polynomial was determined by the minimum RMS value of the prediction error. The polynomials have 125 terms for the wave drag coefficient ($C_{D_{wave}}$) response surface model, 50 terms for the lift curve slope (C_{L_α}), and 40 terms for the leading edge suction term (C_T/C_L^2) response surface models. Both the lift curve slope and the leading edge suction term response surface models contain primarily wing planform related design variables and their interaction terms. The wave drag response surface model contains, in addition to the wing planform variables, other terms which affect the value of the wave drag coefficient. These are most of the fuselage design variables, the horizontal and vertical tail size design variables, and the engine thrust, along with their second order interactions.

Table 2 lists the errors for all generated drag components' response surface models. Comparison of the prediction errors indicates that using RSM to model components of the drag coefficient produced slightly lower errors than using one RS model to approximate the range directly.

5. Optimization Results

5.1. "Standard" Optimization

Results of optimization runs with RS models are compared to the so-called "standard" optimization performed without the RS approximations using the variable-complexity methodology (Section 2.3) developed earlier for the HSCT design problem. The optimization problem formulation in all optimization runs of this work was identical to that of the Case 29c optimization from Ref. [13]. Thus, this optimization run was chosen as a benchmark for comparing the results of using RS models in optimization and is hereafter referred to as the "standard" optimization.

Later analysis indicated that the optimum design of the standard optimization was outside of the limits on the design variables used for the generation of the RS models. Extension of the design space was required later to include the "standard" optimum into the valid RSM region (Section 5.5).

5.2. Unrestricted Design Space Optimization

First, the HSCT optimization was done with the range RS model providing information to the optimizer about the range of the aircraft. The extra constraints listed in Table 1, which were used to identify reasonable designs, were used when optimizing with response surface models. No side constraints on the design variables were used. The optimization was started from the baseline design and stopped after 15 cycles. Figure 4 shows convergence history plots of the actual range, range predicted by the RS model, and TOGW for this optimization run.

As one can see from the plot, after cycle 6 the optimizer went outside the region of validity of the RS model and errors increased rapidly. The optimizer was exploiting the weakness of the response surface model in this region, where the predicted range was much higher than the actual value.

Examining the values of the design variables of the final design of this optimization run indicated that the final design was far outside of the box of $\pm 20\%$ perturbations from the baseline design used in the construction of the RS models. Not surprisingly, the accuracy of the range RS model outside of this box was found to be poor. A similar scenario was observed when the drag components' RS models were used in the optimization without side constraints.

5.3. Optimization in a Restricted Domain

Next, explicit bounds were added on the design variables, to limit them to the multi-dimensional box around the baseline design. The limits of the box were defined to be the same as the maximum and minimum values of the design variables for all designs in the data set A, which was used for generating all RS models. This resulted in 58 additional constraints limiting lower and upper values of each design variable.

Recall that the baseline design used for creating the reasonable design space was pushed inside the feasible domain by using optimization with tightened constraints (Section 3.1). This placed it far from the "standard" optimum and the latter was left outside of the limits on the design variables. Thus, optimization with the side constraints at this stage of the work was aimed at controlling the prediction error of the RS models, rather than capturing the "standard" optimum.

5.3.1. Range RS Model in a Restricted Domain

Figure 5 shows the optimization convergence history of the actual and the RS model range and the TOGW with the box constraints. Note that the range prediction error stabilized at 60–70 n.mi. The final range error for this run is 66.7 n.mi. or 1.21%. Based on previous studies, the amount of fuel required to compensate for a range deficiency is 90 lb/n.mi., so this range error corresponds to a 6003 lb increase in TOGW and brings the TOGW value from 775,792 lb up to 781,795 lb. Some parameters of the final design are listed in Table 3. The final configuration is a relatively light design, although not lighter than the "standard" optimum, which has a TOGW of about 773,000 lb.

5.3.2. Drag Components' RS Models in a Restricted Domain

Using side constraints with the drag RS models again proved to be an effective way of controlling prediction errors, reducing the maximum value of the latter to about 80–90 n.mi. When experimenting with drag RS models, another approach to reducing prediction errors was tested — updating the data set by adding points along the optimization trajectory and regenerating the RS models (see Ref. [12] for more details). Including design points (20 new designs) from previously exploited areas of the design space reduced the prediction errors of the RS models in this region to only 6–10 n.mi., and the optimization converged in 25–30 cycles.

Figure 6 shows optimization convergence plots for this run. The final planform for this run is compared to the baseline and other planforms in Figure 7. Once again, the final configuration is a local optimum with a TOGW value of 818,767 lb, and is considerably heavier than not only the "standard" optimum design, but also than the optimum design for the range RS model optimization. This indicates that the optimizer is still susceptible to getting trapped in local optima due to the nonconvexity of the design space or possibly numerical noise from sources other than high-speed aerodynamics. See Table 3 for a list of major parameters of the final design.

5.4. Comparison of Optimization Results

To clearly see the results of applying RS models in optimization, the convergence histories of the take-off gross weight for three optimization runs — with the range RS model inside a box, with the updated drag RS models inside a box, and a “standard” optimization (Case 29c from [13]) — were compared. Figure 8 compares convergence histories of these runs.

The optimization converged much faster in both runs with RS models — 30 cycles compared to 74 cycles for the “standard” optimization. Also the amplitude of TOGW oscillations is considerably lower for both RSM optimization runs. This is an effect of filtering numerical noise due to the high speed aerodynamics prediction methods by the RS models.

As mentioned earlier, both final designs from the RSM runs are heavier than the one from the “standard” optimization, although the difference in TOGW between the range RS model final design and the “standard” optimum is relatively small. Table 3 lists some parameters of the three designs being compared.

5.5. Optimization Runs with RS Models from “Standard” Optimum

As mentioned before, the “standard” optimum was outside of the box limits of the RS models. Consequently, we extended the limits of the box to include the “standard” optimum, with two hundred new designs generated in the new region and analyzed using high fidelity analysis methods. The new data were included into the RSM data set A, and all RS models were regenerated using this new data set and the old polynomial structure.

Two more optimization runs were started from the “standard” optimum — one with the range RS model and another with the drag RS models. Both optimization runs converged to designs close to the initial design. The TOGW values for both final designs are approximately the same as for the “standard” optimum, with the drag RSM design being slightly lighter (TOGW value corrected for the range deficiency 760,503 lbs), and the range RSM final design being slightly heavier (776,802 lbs). The changes from the “standard” optimum to the RSM optimums can be explained by the slightly different shapes of the approximated response functions compared to the actual response. The inaccuracies of the RS models were within reasonable limits, although only 200 new designs were spread in the new region of the design space. The planforms of all three designs are shown in Figure 9. Table 4 lists some of the parameters of the designs.

6. Conclusions

Response surface methodology has been used to build models for aerodynamic parameters of the HSCT and their use has been investigated. The results show that aerodynamic response surface approximations in high (29) dimensional space can be generated and successfully used in an HSCT optimization, provided that special measures are taken to control the prediction errors of the response surface.

Care must be taken to limit the optimization to regions spanned by the points used in the construction of the RS models. If higher levels of accuracy are required, response surface approximations have to be built in a small region of the design space. This may lead to situations where the optimum design is outside of the region of applicability of the RS models, as was the case with the initial box constraints in this work. Even a relatively large box size (±20% of the baseline values) resulted in the optimum design being outside the box. When this occurs, a moving box approach may be required, where the limits of the box are adjusted and the RS models generated in this new design space.

Using response surface models reduced the amount of numerical noise produced by the expensive analyses during optimization, which in turn improved the convergence of the optimization (25–30 cycles were enough to complete an optimization with response surface models, as opposed to 40–50 cycles without the response surface models). Also, by using response surfaces most of the computational cost is incurred before the actual optimization, providing an opportunity to use high fidelity CFD methods very early in the design process.

Studies also indicated that local optima will exist even with the smooth RS models due to the non-convex design space. With the "standard" optimization procedure utilizing the variable complexity concept we reached the vicinity of the optimum, but because of the noise we could not improve it further. One of the RSM optimization runs managed to improve the optimum reducing the TOGW from 773,000 lb to 761,000 lb. The use of the RSM approach allows us to investigate the details of the design space, including an assessment of the potential local optima, much better.

Questions about the practical reliability of response surface models, their accuracy and prediction capabilities during optimization, and the best choice of starting points (possibly using our previous "standard" method) are still open. Special considerations are needed for ensuring acceptable levels of prediction errors. More research needs to be done on the problem of design space sampling and developing new experimental designs, as D-optimality proved to be computationally expensive in high dimensional problems. Future work will include combining aerodynamic and structural response surface approximations in high dimensions for HSCT optimization.

Acknowledgements

This work has been supported by NASA Grant NAG1-1160 with Mr. P. Coen as contract monitor. Several other graduate students contributed to the work. Two codes developed by Matt Kaufman, *HSCTSearch* and *RSG*, were used here. The *Dopt* code was developed by Dan Haim. Optimization runs and design analyses were done using the *HSCT* code developed by several graduate students: Matt Hutchison, Pete MacMillin, Anthony Giunta, and others.

References

[1] Box, G. E. P. and Wilson, K. B., "On the Experimental Attainment of Optimum Conditions," *Journal of Royal Statistical Society*, vol. B13, pp. 38–45, 1951.

[2] Box, G. E. P., Hunter, W. G., and S., H. J., *Statistics for Experiments: An Introduction to Design, Data Analysis, and Model Building*, pp. 78–83. New York, N. Y.: John Wiley & Sons, 1978.

[3] Myers, R. H. and Montgomery, D. C., *Response Surface Methodology: Process and Product Optimization Using Designed Experiments*, pp. 650–651. New York, N. Y.: John Wiley & Sons, 1995.

[4] Montgomery, D. C., *Design and Analysis of Experiments*, pp. 180–263,340–364. New York, N. Y.: John Wiley & Sons, 1976.

[5] Powers, S. A., "Drag Minimization Using Exact Methods," *AIAA Journal*, vol. 2, pp. 941–943, May 1964.

[6] Tai, J. C., Mavris, D. N., and Schrage, D. P., "Application of a Response Surface Method to the Design of Tipjet Driven Stopped Rotor/Wing Concepts," AIAA 95-3965, Sept 1995. *1st AIAA Aircraft Engineering, Technology, and Operations Congress*, Los Angeles, CA,.

[7] Sellar, R. S., Batill, S. M., and Renaud, J. E., "Response Surface Based, Concurrent Subspace Optimization for Multidisciplinary System Design," AIAA Paper 96-0714, *34th Aerospace Sciences Meeting and Exhibit*,Reno, NV, Jan. 1996.

[8] Engelund, W. C., Stanley, D. O., Lepsch, R. A., and McMillian, M. M., "Aerodynamic Configuration Design Using Response Methodology Analysis," AIAA 93-3967, Aug 1993. *AIAA Aircraft Design, Systems, and Operations Meeting*, Monterey, CA,.

[9] Giunta, A. A., Dudley, J. M., Grossman, B., Haftka, R. T., Mason, W. H., and Watson, L. T., "Noisy Aerodynamic Response and Smooth Approximations in HSCT Design," AIAA Paper 94-4376, Sept. 1994.

[10] Giunta, A., Balabanov, V., Haim, D., Grossman, B., Mason, W., Watson, L., and Haftka, R., "Wing Design for a High-Speed Civil Transport Using a Design of Experiments Methodology," AIAA Paper 96-4001, Proceedings of the *6th AIAA/NASA/ISSMO Symposium on Multidisciplinary Analysis and Optimization*, pp. 168–183, Sept. 1996. http://www.aoe.vt.edu/mad/Publications/96/papers96.html.

[11] Giunta, A. A., "Aircraft Multidisciplinary Design Optimization Using Design of Experiments Theory and Response Surface Modeling Methods," Tech. Rep. MAD 97-05-01, VPI&SU, Blacksburg, VA, May 1997.

[12] Golovidov, O., "Variable-Complexity Response Surface Approximations for Aerodynamic Parameters in HSCT Optimization," Tech. Rep. MAD 97-06-01, VPI&SU, Blacksburg, VA, June 1997, http://www.aoe.vt.edu/mad/Publications/reports/97/MAD970601.pdf.

[13] MacMillin, P., Golovidov, O., Mason, W., Grossman, B., and Haftka, R., "Trim, Control and Performance Effects in Variable-Complexity High-Speed Civil Transport Design," Tech. Rep. MAD 96-07-01, VPI&SU, Blacksburg, VA, July 1996, http://www.aoe.vt.edu/mad/Publications/reports/96/rep1.html.

[14] MacMillin, P. E., Golovidov, O. B., Mason, W. H., Grossman, B., and Haftka, R. T., "An MDO Investigation of the Impact of Practical Constraints on an HSCT Optimization," AIAA Paper 97-0098, Jan. 1997.

[15] Hutchison, M., Unger, E., Mason, W. H., Grossman, B., and Haftka, R., "Variable-Complexity Aerodynamic Optimization of an HSCT Wing Using Structural Wing-Weight Equations," AIAA Paper 92-0212, Jan. 1992.

[16] Hutchison, M. G., Unger, E. R., Mason, W. H., Grossman, B., and Haftka, R. T., "Variable-Complexity Aerodynamic Optimization of an HSCT Wing Using Structural Wing-Weight Equations," *Journal of Aircraft*, vol. 31, no. 1, pp. 110–116, 1994.

[17] Dudley, J., Huang, X., MacMillin, P. E., Grossman, B., Haftka, R. T., and Mason, W. H., "Multidisciplinary Optimization of the High-Speed Civil Transport," AIAA 95-0124, Sept 1995. *33rd Aerospace Sciences Meeting and Exhibit.* Reno, NV.

[18] Grandhi, R. V., Thareja, R., and Haftka, R. T., "NEWSUMT-A: A General Purpose Program for Constrained Optimization Using Approximation," *ASME Journal of Mechanisms, Transmissions and Automation in Design*, vol. 107, pp. 94–99, 1985.

[19] Hutchison, M. G., Huang, X., Mason, W. H., Haftka, R. T., and Grossman, B., "Variable-Complexity Aerodynamic-Structural Design of a High-Speed Civil Transport Wing," AIAA Paper 92-4695, Sept. 1992.

[20] Hutchison, M. G., Unger, E., Mason, W. H., Grossman, B., and Haftka, R. T., "Variable-Complexity Aerodynamic Optimization of a High Speed Civil Transport Wing," *Journal of Aircraft*, vol. 31, pp. 110–116, Jan.-Feb. 1994.

[21] Hutchison, M. G., Mason, W. H., Grossman, B., and Haftka, R. T., "Aerodynamic Optimization of an HSCT Configuration Using Variable-Complexity Modeling," AIAA Paper 93-0101, Jan. 1993.

[22] Bertin, J. and Smith, M., *Aerodynamics for Engineers*, pp. 261–282. Prentice Hall, 2nd ed., 1989.

[23] Carlson, H., Mack, R., and Barger, R., "Estimation of Attainable Leading Edge Thrust for Wings at Subsonic and Supersonic Speeds," NASA TP-1500, 1979.

[24] Carlson, H. and Miller, D., "Numerical Methods for the Design and Analysis of Wings at Supersonic Speeds," NASA TN D-7713, 1974.

[25] Harris, Jr., R. V., "An Analysis and Correlation of Aircraft Wave Drag," NASA TM X-947, 1964.

[26] Hutchison, M. G., *Multidisciplinary Optimization of High-Speed Civil Transport Configurations Using Variable-Complexity Modeling.* Ph.D. dissertation, Virginia Polytechnic Institute and State University, Blacksburg, Virginia, Mar. 1993.

[27] Cohen, D. and Friedman, M. D., "Theoretical Investigation of the Supersonic Lift and Drag of Thin, Sweptback Wings with Increased Sweep near the Root," NACA TN-2959, June 1953.

[28] Kaufman, M. D., "Variable-Complexity Response Surface Approximation for Wing Structural Weight in HSCT Design," Master's thesis, Virginia Polytechnic Institute and State University, Blacksburg, Virginia, Apr. 1996. http://scholar.lib.vt.edu/theses/public/etd-24012559631561/etd-title.html.

[29] Kaufman, M., Balabanov, V., Burgee, S., Giunta, A., Grossman, B., Haftka, R., Mason, W., and Watson, L., "Variable-complexity response surface approximations for wing structural weight in HSCT design," *Computational Mechanics*, vol. 18, pp. 112–126, June 1996.

[30] Hinkelmann, K., *Design and analysis of experiments.* New York, N. Y.: John Wiley & Sons, Inc., 1994.

[31] Box, M. J. and Draper, N. R., "Factorial Designs, the $|\mathbf{X}^T\mathbf{X}|$ Criterion, and Some Related Matters," *Technometrics*, vol. 13, no. 4, 1971.

[32] Mitchell, T., "An Algorithm for the Construction of D-Optimal Experimental Designs," *Technometrics*, vol. 16, no. 2, 1974.

[33] Anderson, E., Bai, Z., Bischof, C., Demmel, J., Dongarra, J., Du Coz, J., Greenbaum, A., Hammarling, S., McKenney, A., and Sorensen, D., *LAPACK User's Guide.* Philadelphia: Society for Industrial and Applied Mathematics, 1992.

Table 1: Criteria for reasonable designs

#	Description[a].
1-34	HSCT geometric constraints
35-36	20,000 lbs $< W_{b_F} <$ 120,000 lbs
37-58	Minimum fuselage radius
59	Inboard $\Lambda_{le} >$ outboard Λ_{le}
60	$\Lambda_{le} > 0$
61-62	5,000 ft^2 $< S_w < 15,000$ ft^2
63-64	$1.0 < AR < 3.2$
65	Inboard $\Lambda_{te} < 40°$
66-83	$c_{y_{i+1}}/c_{y_i} < 1.0$
84	Approximate range > 5,000 n. mi.
85-86	0.8×thrust required < thrust available (approximate analysis)

[a]Symbols in the table are: W_{b_F} — wing bending matarial weight; Λ_{le} — leading edge sweep angle; AR — wing aspect ratio; Λ_{te} — wing trailing edge sweep angle; S_w — wing area; c_{y_i} — wing section lift coefficient.

Table 2: Errors of created RS models for range and drag components. The last row shows range prediction errors using the drag RS models.

Parameter	Average error	RMS error	Typical value
Range	11.1 n.mi.	17.5 n.mi	5500 n.mi.
$C_{D_{wave}}$	0.12×10^{-4}	0.20×10^{-4}	18×10^{-4}
C_{L_α}	0.00095	0.0020	1.6
C_T/C_L^2	0.00033	0.00093	0.12
Range[a]	8.2 n.mi.	11.3 n.mi.	5500 n.mi.

[a]Predicted using the drag RS models.

Table 3: Comparison of the three optimum designs from RS model optimization runs and a “standard” optimization (Case 29c from [13]).

Parameter	Baseline design	Range RS model	Drag RS models	“Standard” optimization
Gross Weight (*lbs*)	876,488	775,792	818,767	772,981
Corrected Gross Weight (*lbs*)	873,419	781,795	817,795	772,752
Fuel Weight (*lbs*)	464,743	397,121	433,595	403,345
Fuel Wt / Gross Wt	53.0%	51.1%	53.0%	52.2%
Wing Area (ft^2)	14,157	13,992	13,081	13,191
Aspect Ratio	2.22	1.76	2.06	1.99
Wing thickness at root, %	2.81	2.26	2.84	2.37
Vertical Tail Area (ft^2)	921.1	852.0	895.0	454.1
Horizontal Tail Area (ft^2)	1,973.2	1,914.0	1,761.4	1,494.4
Nacelle 1 position, y (*ft*)	11.5	9.2	9.5	7.1
Nacelle 2 position, y (*ft*)	28.3	33.9	33.5	14.4
Range actual (*n.mi.*)	5,534.1	5,434.3	5,510.8	5,503.0
Range RSM (*n.mi.*)	5,526.0	5,501.0	5,500.5	n/a
Landing angle of attack	10.3°	11.1°	11.0°	10.6°

Table 4: Comparison of the final designs for RS model optimization runs started from “standard” optimization optimum (Case 29c from [13]).

Parameter	Range RS model	Drag RS models	“Standard” optimization
Gross Weight (*lbs*)	773,112	753,303	772,981
Corrected Gross Weight (*lbs*)	776,802	760,503	772,752
Fuel Weight (*lbs*)	401,726	387,763	403,345
Fuel Wt / Gross Wt	51.7%	50.9%	52.2%
Wing Area (ft^2)	13,809	12,675	13,191
Aspect Ratio	2.05	2.07	1.99
Wing thickness at root, %	2.41	2.40	2.37
Vertical Tail Area (ft^2)	460.0	454.0	454.1
Horizontal Tail Area (ft^2)	1,516.8	1,484.6	1,494.4
Nacelle 1 position, y (*ft*)	7.0	7.0	7.1
Nacelle 2 position, y (*ft*)	14.5	14.7	14.4
Range actual ($n.mi.$)	5,468.8	5,420.4	5,503.0
Range RSM ($n.mi.$)	5,500.1	5,500.3	n/a
Landing angle of attack	10.6°	10.6°	10.6°

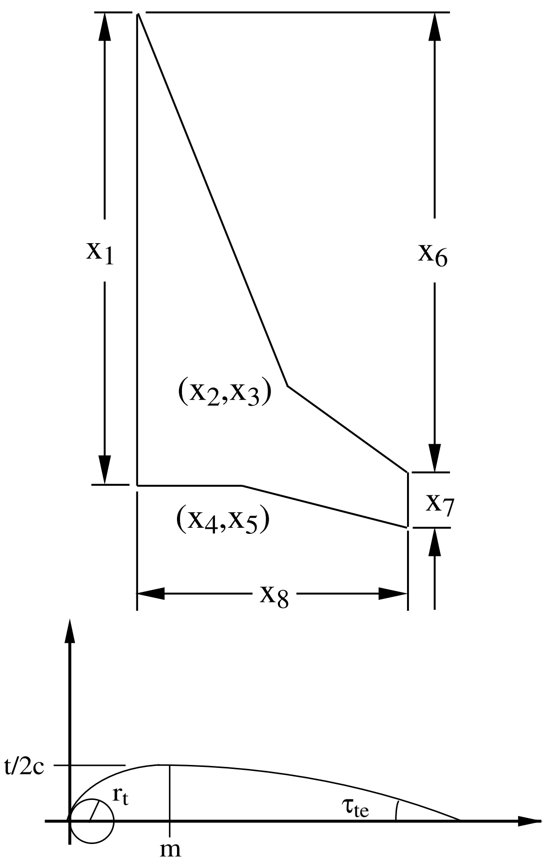

Figure 1: HSCT wing planform and airfoil parameters.

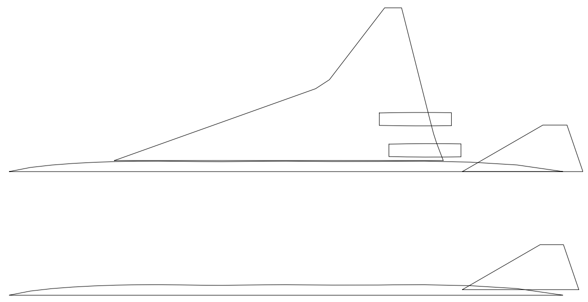

Figure 2: Baseline HSCT design.

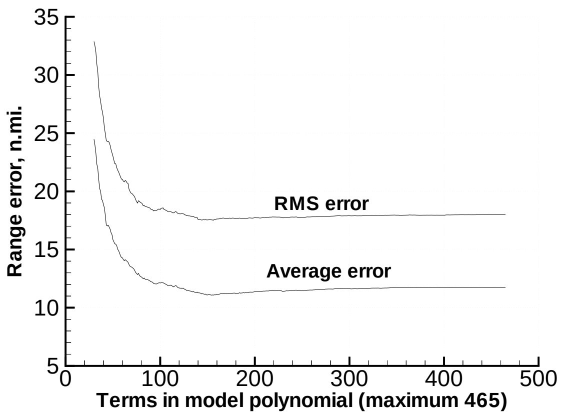

Figure 3: Range response surface model prediction errors (computed at the design points of set B) versus number of terms in the model polynomial.

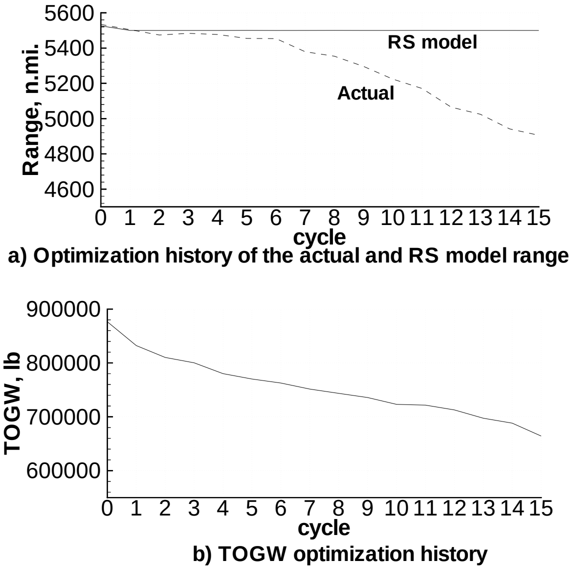

Figure 4: Optimization history plots of actual and RS model range and TOGW for unrestricted optimization run with the range RS model.

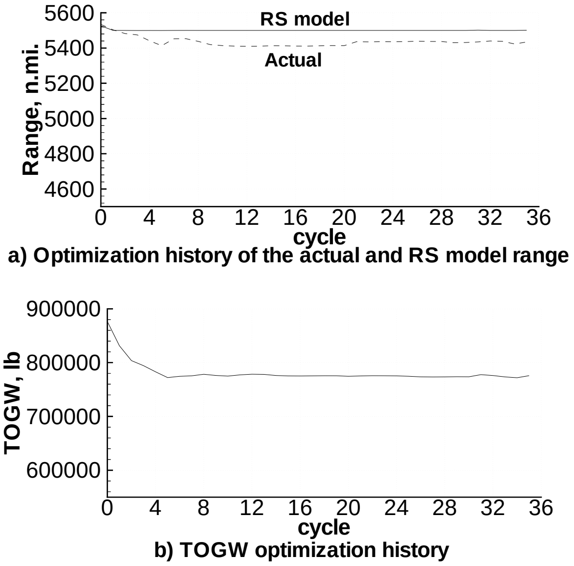

Figure 5: Optimization history plots of actual and RS model range and TOGW for optimization run with the range RS model inside a box.

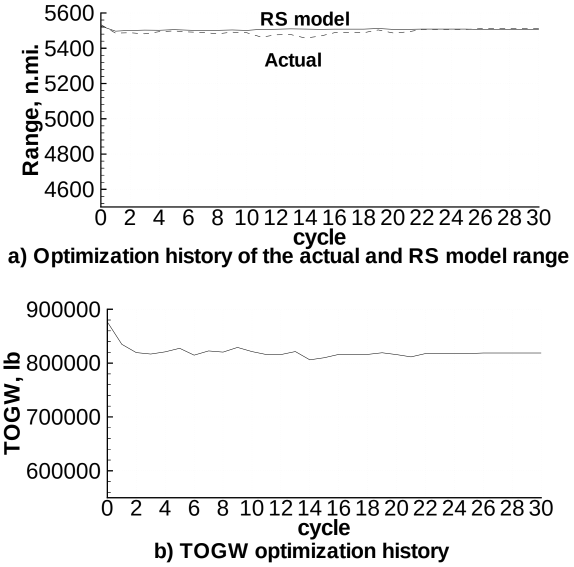

Figure 6: History plots of optimization with updated drag RS models inside a box.

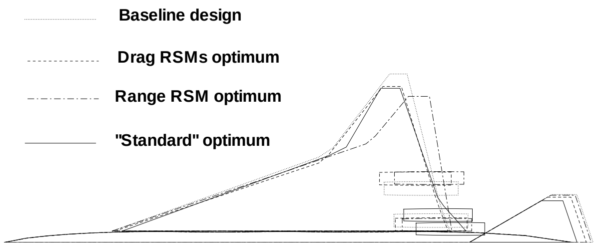

Figure 7: Baseline and final planforms for 3 optimization runs.

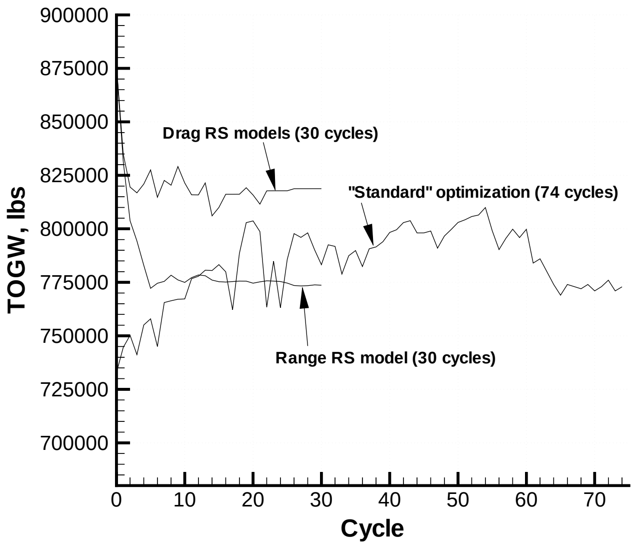

Figure 8: Convergence histories of TOGW for three optimization runs.

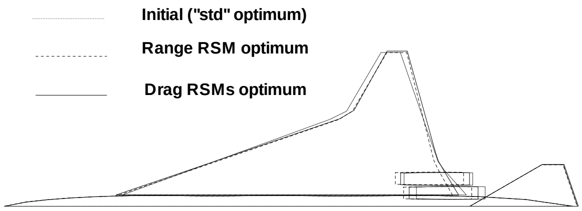

Figure 9: Final planforms of optimization runs with RS models from "standard" optimum.